Biointerfrence between Zinc Oxide/Alginate Nanocomposites and Freshwater Bivalve

Article *in* Biointerface Research in Applied Chemistry · July 2022

DOI: 10.33263/BRIAC133.277

Biointerface Research in Applied Chemistry
Open-Access Journal (ISSN: 2069-5837)

Article
Volume 13, Issue 3, 2022, 277
https://doi.org/10.33263/BRIAC133.277

Biointerfrence between Zinc Oxide/Alginate Nanocomposites and Freshwater Bivalve

Tahani Younis Omar [1], Habiba Ihab Ahmed Elshenawy [2], Marwa Ahmed Abdelfattah [3], Abdeljalil Mohamed Al Shawoush [3], Ayman Saber Mohamed [3,*], Dalia Y. Saad [3]

1 Zoology Department, Faculty of Science, Sirte University, Sirte, Libya; dr.tahani1972@yahoo.com (T.Y.O.);
2 Faculty of Biotechnology, October University for Modern Sciences and Arts (MSA), Egypt; habibaihab49@gmail.com (H.I.A.E.);
3 Zoology Department, Faculty of Science, Cairo University 12613, Giza, marwaahmedabdelfattah77@gmail.com (M.A.A.); sedra200713@yahoo.com (A.M.A.S.); ayman81125@hotmail.com (A.S.M.); dyossri@gmail.com (D.Y.S.);
* Correspondence: ayman81125@cu.edu.eg (A.S.);

Scopus Author ID 56564677600
Received: 20.04.2022; Accepted: 16.05.2022; Published: 10.07.2022

Abstract: Commercial usage of zinc oxide nanoparticles threatens the aquatic ecosystem. The green synthesis of ZnO nanoparticles is an environmentally benign method of nanoparticle manufacture. Aim: In the current study, freshwater bivalves were employed as a crucial indicator for the green synthesis of alginate/ZnO nanocomposite. Transmission electron microscopy, ultraviolet spectroscopy, and X-Ray diffraction were used to analyze the produced Alginate/ZnO nanocomposite. The bivalve was subjected to various dosages of ZnO and alginate/ZnO nanoparticles (12, 25, and 50 mg/L). The alginate/ZnO nanocomposite size was between (10-15 nm), whereas ZnO was between (5-10 nm). Malondialdehyde and nitric oxide levels increased at all Alginate/ZnO nanocomposite doses, whereas catalase and glutathione levels decreased in all organs. After exposure to alginate/ZnO nanocomposite nanoparticles, the gills and mantle histopathological examinations revealed changes. Incorporating alginate into the production of ZnONPs causes combinatorial harmful effects in *Coelatora aegyptica*, including oxidative stress and histopathological alterations. *Coelatora aegyptiaca* was found to be a sensitive bio-indicator for nanoparticle-induced water pollution.

Keywords: *Coelatora aegyptiaca*; zinc oxide; sodium alginate; water pollution; nanoparticles; oxidative stress.

1. Introduction

In recent years, producing zinc oxide nanoparticles with precise shape and morphology has piqued interest in fundamental research and industrial applications. A variety of typical processes for producing zinc oxide nanoparticles were applied, including hydrothermal, sol-gel, microwave, and precipitation [1-3]. On the other hand, some synthetic techniques have many disadvantages since they need numerous long and complicated procedures to make pure nanomaterials. Nanoparticles (NPs) made of polymeric materials have been widely exploited in developing new medication delivery methods. Encapsulated compounds are becoming more popular due to their better physical and chemical stability, lack of toxicity, potential to increase bioavailability, and ability to administer encapsulated drugs in a targeted manner [4]. Alginate has been studied extensively as a natural polymer for producing polymeric nanoparticles (NPs)

[5]. Sodium alginate is a water-soluble alginic acid polysaccharide salt with anti-tumor, immune-regulating, non-toxic, biodegradable, and high biocompatibility properties [6].

Incorporating nanotechnologies into a wide range of produced items raises concerns about releasing artificial nanoparticles into the environment [7]. Their unusual physicochemical features, strong penetrating ability, broad surface area, and chemical activity make them appealing for industrial and medicinal applications and potentially damaging the environment and living species [8]. During manufacture, usage, discharge, treatment, and deposition, nanoparticles are released into marine and freshwater environments in massive amounts [9]. The impact of nanoparticles on aquatic and terrestrial systems has recently gotten much attention [10].

Observable changes in cellular or biochemical processes, structures, or components, caused by xenobiotics, illness, or other physical agents are known as biomarkers (or biological markers) [11]. Because they are known to concentrate these elements, bivalves are utilized as bioindicators of heavy metal pollution, giving a time-integrated signal of environmental contamination [12]. *Caelatura aegyptiaca* is a Molluscan Bivalve belonging to Unionidae widely distributed along the Nile from Assiut to Damietta branches [13]. In the current study, freshwater bivalves were employed as a crucial indicator for the green synthesis of alginate/ZnO nanocomposite.

2. Material and Methods

2.1. Chemicals and materials.

Sodium Alginate, zinc acetate, and sodium hydroxide (NaOH) were purchased from (Sigma Aldrich, USA).

2.2. Synthesis of zinc oxide nanoparticles (ZnO NPs).

According to Cao et al. [14], the synthesis of ZnO NPs was, in brief, 7.22 mmol of NaOH dissolved in 320 μL of bi-distilled water and then in 25 mL of ethanol was added dropwise to 3.73 mmol of zinc acetate dihydrate dissolved in 40 ml of ethanol. After 2 hours of vigorous and steady stirring at 60 degrees Celsius, the solution was allowed to cool to ambient temperature. Then ZnO samples were collected by centrifugation and washed thoroughly with pure fresh ethanol. ZnO NPs were re-dispersed in ethanol or dried at 60 ^{o}C for two hours.

2.3. Synthesis of zinc oxide/alginate nanocomposites (ZnO/Alg NC).

To make alginate gelation, a stirrer was used to combine sodium alginate solution (3%) with zinc acetate solution (5%) to get a homogenous mixture, followed by filtration. The resulting hydrogel was rinsed multiple times with distilled water to eliminate any remaining Zinc acetate. The gel was then dried overnight in a 60 ^{o}C oven to eliminate moisture. To achieve the final product of nano-scale zinc oxide, the dried gel was calcined in an oven at 500 ^{o}C for 3 hours [15].

2.4. Characterization of ZnONPs and ZnO/Alg NCs.

Transmission electron microscopic (A JEOL JEM-2100) have been used to examine the nanostructure of ZnONPs and ZnO/Alg NCs.

ZnONPs and ZnO/Alg NCs were characterized using an aqueous solution and a UV-visible spectrophotometer (Shimadzu UV-1601) operating at a 10 nm interval in the wavelength range 200-700 nm.

The structure of the generated particles was determined using an X-ray diffractometer (XRD-6000, Shimadzu, Japan) operating at 40 kV and 30 mA with Cu K radiation (wavelength - 0.15406 nm).

2.5. Experimental animals.

Coelatura aegyptiaca (shell length 11− 14 cm & width 6.5–8.5) have been from the Nile River in Abu Rawash area, Giza Governorate, Egypt. The animals were transferred to the laboratory at once ad added to a glass-reinforced plastic (FRP) tank at room temperature. During the study, the animals were fed with commercial phytoplankton.

2.6. Experimental design.

Three different concentrations of ZnO NPS and ZnO/Alg NCs were selected in the present study (12.5, 25, and 50 mg/ L). They were sonicated for 20 minutes in dechlorinated waters. Mussels (5 animals/concentration level) exposed to ZnO NPS and ZnO/Alg NCs for seven days. A control group of mussels was maintained in dechlorinated freshwater.

2.7. Determination of ZnONPs concentration.

ZnO concentrations were determined using ICP-OES equipment (iCAP 6500 Duo, Thermo Scientific, Cambridge, UK) at 213.856 nm. Before the measurement, 20 minutes of sonication were performed. The analyses were performed in triplicates.

2.8. Samples tissue preparation for biochemical analysis.

Soft tissues (mantle, foot, digestive gland, and gills) were removed and washed with ice-cold saline (0.9 %). The tissues were homogenized (10% w/v) in an ice-cold 50 mM phosphate buffer (pH 7.4). The homogenate was centrifuged for 15 minutes at 3000 rpm at 4°C, and the supernatant was utilized for biochemical analysis [16,17].

2.9. Assessment of oxidative stress markers.

The tissue's supernatant homogenate was used to measure oxidative stress indicators. Biodiagnostic kits (Biodiagnostic Dokki, Giza, Egypt) were used for the determination of lipid peroxidation, which was measured by the formation of malondialdehyde (MDA) [13], glutathione (GSH) [18], catalase [19] and nitric oxide (NO) [20].

2.10. Histopathological examination.

Dissected gills and mantle tissues were fixed in 10% neutral-buffered formalin. An automated processor was used to wash, dehydrate, and embed the preserved specimens in paraffin wax (58–60°C). Paraffin blocks were trimmed to a suitable size, and tissues were cut using a microtome 4–5 µm thickness. Following deparaffinization, slides were rehydrated and stained with hematoxylin and eosin [21,22].

2.11. Statistical analysis.

Values were expressed as means ±SE. Within-group comparisons were assessed using one-way analysis of variance (ANOVA) with Duncan post hoc test to compare group means, with $p < 0.05$ regarded as statistically significant. The statistical analysis was performed using SPSS for Windows (version 15.0).

3. Results and Discussion

3.1. Characterization of synthesized nanoparticles.

TEM investigation revealed the synthesis of sodium alginate/ZnO NCs and ZnO NPs in size ranges of 10–15 nm and 10-5 nm, respectively. The produced nanoparticles have a nearly spherical shape (Figure 1).

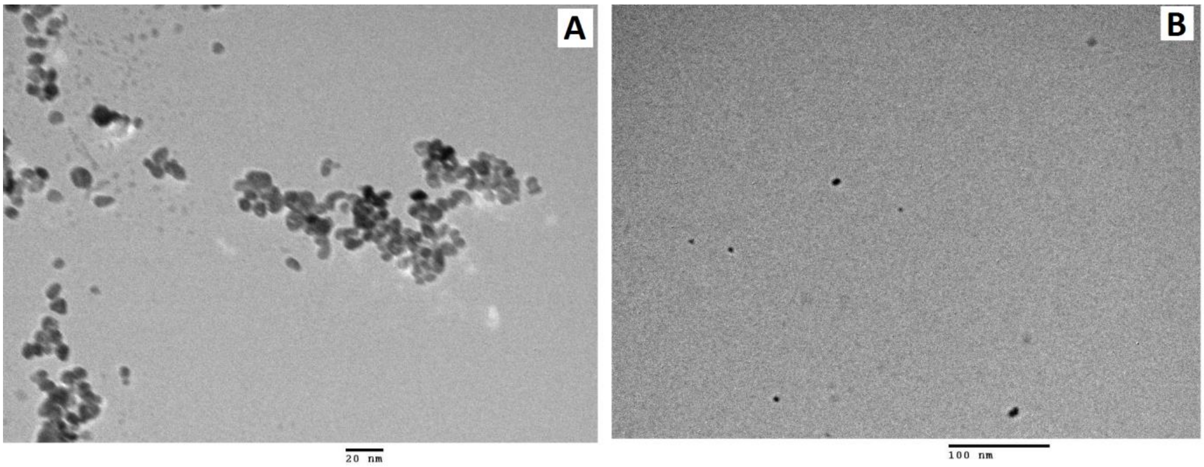

Figure 1. TEM micrographs of (**A**) ZnO NPs, and (**B**) ZnO/Alg NCs.

As shown in Figure 2**,** the maximum UV spectra of sodium alginate/ZnO NCs and ZnO NPs were 315 and 370 nm, respectively, which attributed to the intrinsic band-gap of Zn-O absorption.

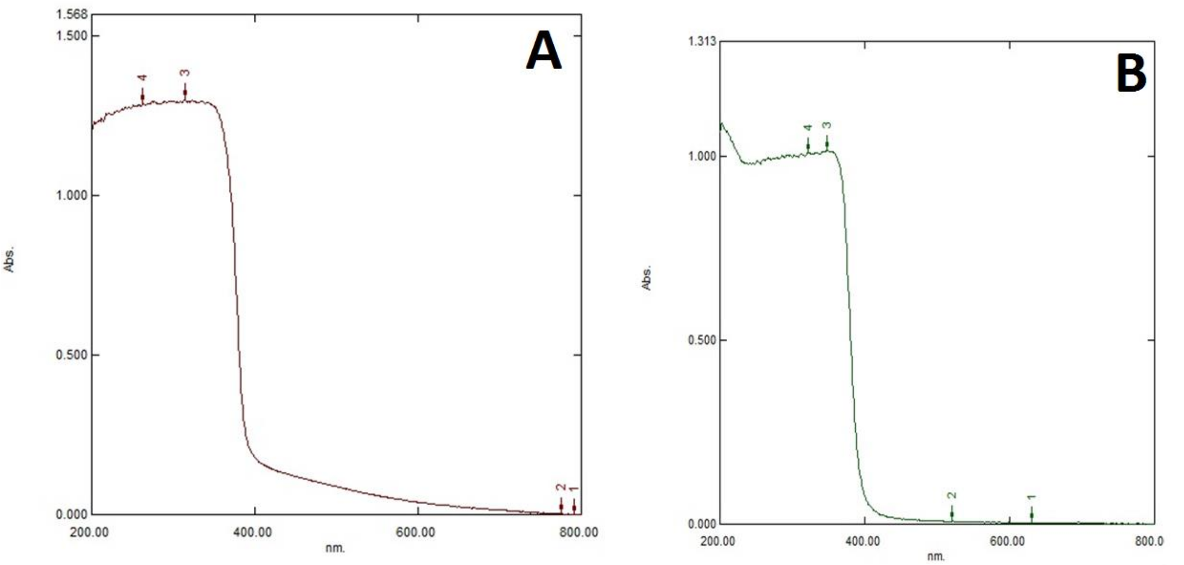

Figure 2. UV–vis absorption spectrum of (**A**) ZnO NPs and (**B**) ZnO/Alg NCs.

The crystalline structure of the produced ZnONPs and ZnO/Alg NCs was determined using X-ray diffraction analysis. Diffraction peaks were visible in the XRD spectrum of ZnO/Alg NCs at two values of 32.7, 34.5, 36.4, and 47.7. ZnONPs, on the other hand, showed diffraction peaks at two values of 31.8, 34.5, 36.3, and 47.5, with a broadening of the peaks (Figure 3).

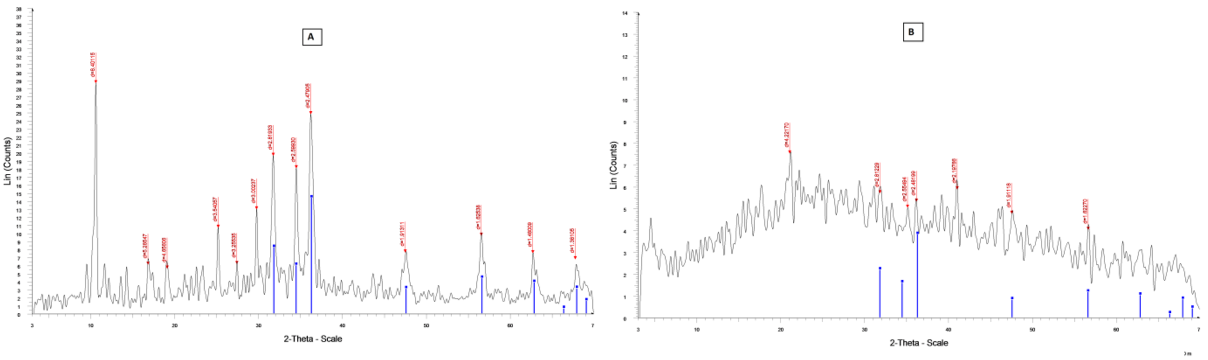

Figure 3. X-ray diffractometer (XRD) analysis of (**A**) ZnO NPs, and (**B**) ZnO/Alg NCs.

3.2. ZnONPs concentration.

The measured concentrations of ZnO in the ZnO-agar nanocomposite solution were 46.25, 23.11, and 11.08 mg/L for each exposed concentration of 50, 25, and 12.5 mg/L, respectively (Figure 4).

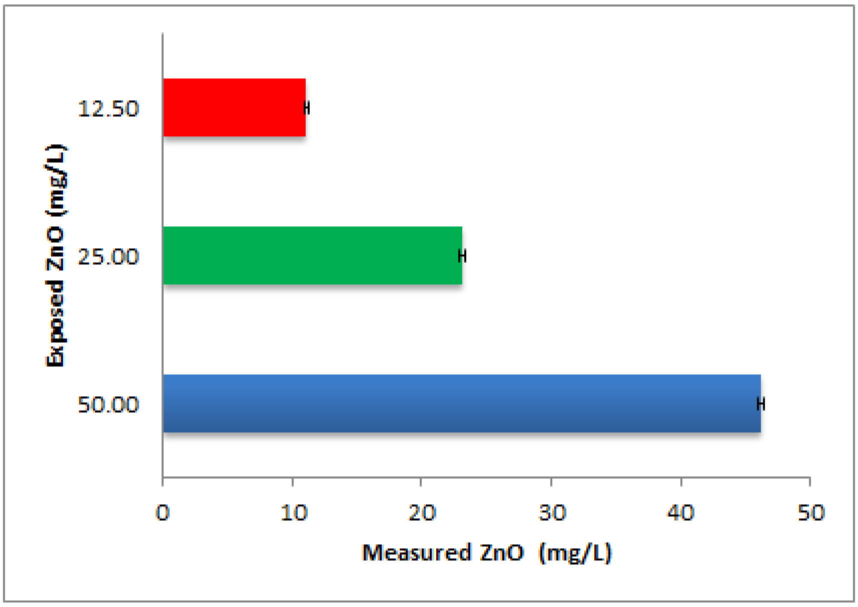

Figure 4. ZnO concentration in ZnO/Alg NCs (n=3 for each concentration).

3.3. Effect of ZnO/Alg NCs, and ZnO NPCs on the oxidative status.

Water contamination has long been seen as a severe threat to all aquatic ecosystems. Despite their widespread usage in several applications, the toxicity of heavy metal nanoparticles to aquatic creatures has not been adequately investigated, posing a health risk [23-25]. ZnO NPs are one of the most damaging NPs in the aquatic environment [26]. The presence of oxidative stress in most biological systems has been identified as the principal cytotoxic effect of ZnO NPs.

Furthermore, ZnO NPs accumulating in bodily tissues may cause hazardous effects. The heterogeneity in size and quantity of ZnO NPs produced by several industrial sites has had an ecological influence on the aquatic environment [27]. Many NPs exhibit oxidant properties, such as the potential to generate reactive oxygen species (ROS) or block the antioxidant system of cells, resulting in oxidative stress [28]. According to Abdel-Halim, oxidative stress is a regularly described mechanism of nanoparticle toxicity. Oxidative stress was created by an imbalance between reactive oxygen species (ROS) production and the body's antioxidant defense capacity [29,30].

MDA concentration in the mantle increased significantly ($P<0.05$) in the ZnO NPs and ZnO/Alg NCs concentration groups compared to the respective control groups. ZnO/Alg NCs had a substantial increase ($P<0.05$) in mantle MDA content as compared to the ZnO group (Table 1). MDA is a highly reactive metabolic product produced in tissues due to a chain reaction combining lipid peroxide and free oxygen radicals [31,32].

Table 1. Effect of different ZnONPS and ZnO/Alg NCs on MDA concentration (nmol/g.tissue) in *Coelatura aegyptiaca* organs.

Group	Concentration (mg/L)	Organ			
		Mantle	Foot	Digestive gland	Gills
Control	0	0.72± 0.13^{a}	0.42 ± 0.06 ^{a}	2.93 ± 0.07 ^{f}	1.19± 0.11 ^{a}
ZnO	12.5	0.75 ± 0.09^{a}	1.10 ± 0.03 ^{b}	0.69± 0.03 ^{a}	1.90± 0.12 ^{b}
	25	0.78 ± 0.09^{a}	1.59 ± 0.09 ^{c}	0.81± 0.03 ^{b}	2.65 ± 0.81 ^{c}
	50	1.12 ± 0.1^{b}	1.95 ± 0.10 ^{d}	1.07± 0.03 ^{c}	3.35 ± 0.07 ^{d}
ZnO-Alg	12.5	1.19 ± 0.06^{b}	1.34 ± 0.13 ^{b}	1.21 ± 0.04 ^{c}	3.26 ± 0.12 ^{d}
	25	1.66 ± 0.2^{c}	1.61 ± 0.13 ^{e}	1.94 ± 0.05 ^{d}	3.57± 0.05 ^{d}
	50	1.61± 0.13^{c}	3.0 ± 0.07 ^{c}	2.60 ± 0.02 ^{e}	3.93 ± 0.22 ^{c}

Values are means ± se (n = 5 per group). Each value not sharing a common letter superscript is significantly different ($P <0.05$).

A significant increase ($P<0.05$) in NO concentration was found in both tested groups of ZnO NPs and ZnO/Alg NCs compared to the control group, as shown in Table 2. Also, a significant increase in ZnO/Alg NCs group was found compared to the ZnO NPs in a concentration-dependent manner ($P<0.05$). NO is involved in oxidative stress and illness, and its generation by nitric oxide synthases (NOS) is controlled in various normal physiological activities [33]. However, increased NO concentration indicates that ZnO/Alg NCs boosted NOS activity and increased NO generation to counteract the stress caused by nanoparticle exposure [34,35].

Table 2. Effect of different ZnONPS and ZnO/Alg NCs on NO concentration (µM/g.tissue) in *Coelatura aegyptiaca* organs.

Group	Concentration (mg/L)	Organ			
		Mantle	Foot	Digestive gland	Gills
Control	0	5.31 ± 0.43^{a}	12.99 ± 0.63^{a}	4.44± 0.37^{a}	7.21 ± 0.63^{a}
ZnO	12.5	7.43 ± 0.37^{b}	16.27 ± 0.60^{b}	7.02 ± 1.39^{b}	11.03 ± 0.82^{b}
	25	13.67 ± 0.79^{c}	22.93 ± 0.67^{c}	12.74 ± 0.36^{c}	17.96 ± 1.03^{c}
	50	15.96 ± 0.55^{d}	29.86±	16.11 ±	21.81 ±

Group	Concentration (mg/L)	Organ			
		Mantle	Foot	Digestive gland	Gills
			0.67[d]	0.41[d]	1.19[d]
ZnO-Alg	12.5	9.02 ± 0.57[b]	21.50 ± 0.81[c]	8.00 ± 0.56[b]	12.71 ± 0.65[b]
	25	16.33 ± 0.68[d]	29.10 ± 0.91[d]	13.43 ± 0.24[c]	18.77 ± 0.68[c]
	50	23.17± 0.76[e]	37.13 ± 0.93[e]	18.20 ± 0.38[e]	28.42 ± 0.95[e]

Values are means ± se (n = 5 per group). Each value not sharing a common letter superscript is significantly different (P <0.05). Statistical analysis was tested by one-way analysis of variance (ANOVA) with the Duncan post hoc test.

GSH showed a significant decrease ($p < 0.05$) in ZnO NPs and ZnO/Alg NCs groups compared to the control group represented in Table 3. The decrease in GSH level within ZnO/Alg NCs group compared to the ZnO NPs in a concentration-dependent manner ($P<0.05$). Furthermore, GSH is one of the most common non-protein thiol antioxidants, and it is engaged in many metabolic pathways critical for cellular homeostasis and oxidative stress defense nanoparticle [29,36]. Cells' adaptive response to oxidative stress is widely assumed to drop GSH levels [37,38].

Table 3. Effect of different ZnONPS and ZnO/Alg NCs on GSH concentration (mg/g.tissue) in *Coelatura aegyptiaca* organs.

Group	Concentration (mg/L)	Organ			
		Mantle	Foot	Digestive gland	Gills
Control	0	3.80± 0.02[e]	3.70 ± 0.17 [e]	2.93± 0.30 [e]	3.36 ± 0.04 [f]
ZnO	12.5	3.41 ± 0.04 [d]	3.22 ± 0.18 [d]	2.66 ± 0.03 [d]	3.26 ± 0.02 [e]
	25	3.26 ± 0.02 [d]	2.80 ± 0.07 [c]	2.27 ± 0.03 [c]	2.81 ± 0.05 [d]
	50	2.49 ± 0.01 [b]	2.47 ± 0.10 [ab]	2.05 ± 0.03 [b]	2.44 ± 0.03 [c]
ZnO-Alg	12.5	2.64 ± 0.07 [c]	2.99 ± 0.15 [c]	2.21 ± 0.04 [c]	2.69 ± 0.02 [d]
	25	2.21± 0.05[b]	2.51 ± 0.16 [a]	1.60 ± 0.05 [b]	2.09 ± 0.02 [b]
	50	1.7 ± 0.01 [a]	2.09 ± 0.10 [a]	1.94 ± 0.02 [a]	1.90 ± 0.01 [a]

Values are means ± se (n = 5 per group). Each value not sharing a common letter superscript is significantly different (P <0.05).

Table 4. Effect of different ZnONPS and ZnO/Alg NCs on CAT activity (U//g.tissue) in *Coelatura aegyptiaca* organs.

Group	Concentration (mg/L)	Organ			
		Mantle	Foot	Digestive gland	Gills
Control	0	27.05 ± 0.14 [g]	12.44 ± 0.70 [d]	15.42 ± 0.91 [e]	28.36 ± 0.96 [f]
ZnO	12.5	22.04 ± 0.18 [f]	7.84 ± 0.27 [c]	10.09 ± 1.08 [d]	22.84 ± 0.74 [e]
	25	17.88 ± 0.19 [e]	5.47 ± 0.50 [a]	7.07 ± 0.16 [c]	8.14 ± 0.35 [b]
	50	9.48 ± 0.19 [d]	5.41 ± 0.21 [a]	5.27 ± 0.33 [b]	5.23 ± 0.23 [a]
ZnO-Alg	12.5	8.04 ± 0.17 [c]	6.79 ±	6.97 ±	16.19 ± 0.58 [d]

Group	Concentration (mg/L)	Organ			
		Mantle	Foot	Digestive gland	Gills
			0.41 [b]	0.04 [c]	
	25	6.45 ± 0.12 [b]	4.83 ± 0.48 [a]	2.87 ± 0.10 [a]	10.45 ± 0.82 [c]
	50	4.51 ± 0.13 [a]	5.17 ± 0.26 [a]	3.49 ± 0.10 [a]	7.22 ± 1.13 [a]

Values are means ± se (n = 5 per group). Each value not sharing a common letter superscript is significantly different (P <0.05).

ZnO NPs and ZnO/Alg NCs decrease CAT activity concentration-dependent compared to the control group, as in Table 4. On the other hand, CAT activity was considerably lower in ZnO/Alg NCs groups compared to ZnO NPs groups. Catalase is an essential enzyme in the defense against reactive oxygen species [39,40]. The reduction in CAT activity might be attributed to a reduction in protein synthesis due to an increase in the peroxidation end product MDA [34]. The reduction in GSH and CAT after exposure to ZnO/Alg NCs might also be explained by the overproduction of ROS produced by NP toxicity.

3.4. Histopathology of gills.

The gills in control animals showed the typical structure of a bivalve ctenidium, consisting of filaments and water channels. Each gill filament consisted of central core tissue, two chitinous rods, and well-arranged epithelial cells, having lateral and frontal cilia (Figure 5). However, exposure of mussels to ZnO NPs and ZnO/Alg NCs for seven days indicated that the lateral and frontal cilia had sloughed off, and the lumen of the gill filaments had wandering blood cells. In addition, the gill filaments were thoroughly disorganized, and the cells were destroyed with enlargement of the gill lumen.

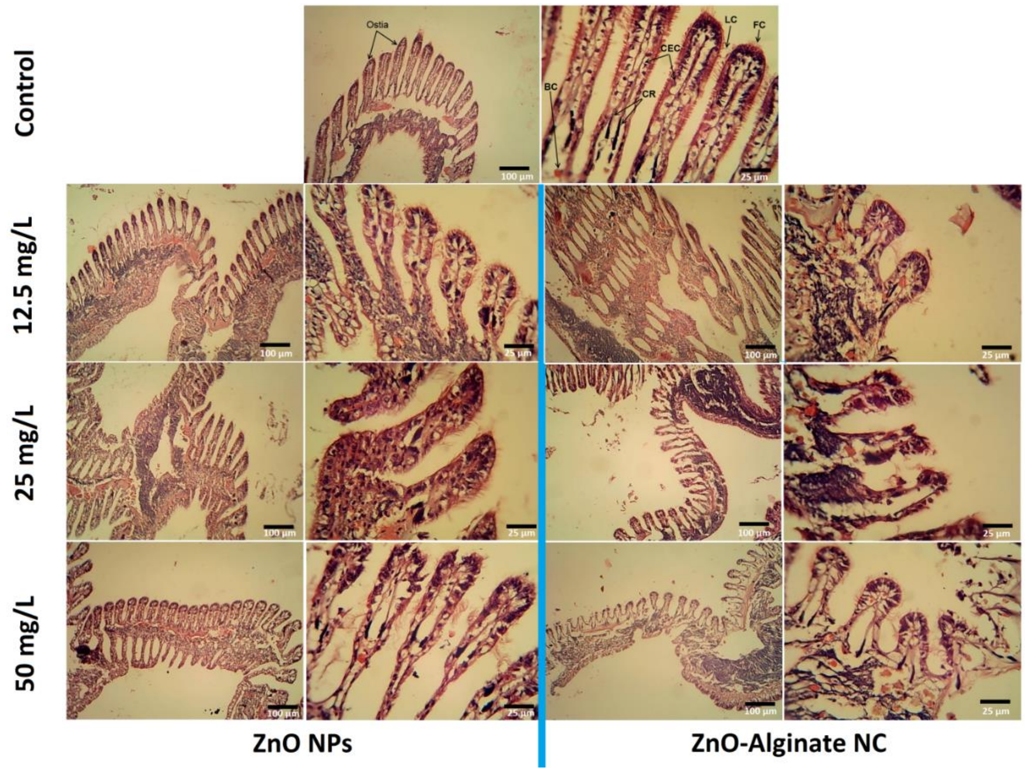

Figure 5. Light micrographs of gills of *Coelatura aegyptiaca* exposed to ZnO NPs and ZnO/Alg NC NCs (H&E). "BC" blood cells, "CEC" ciliated columnar epithelial cells, "CR" chitinous rods. "FC" frontal cilia, and "LC" lateral cilia.

3.5. Histopathology of the mantle.

In the light micrograph of the mantle, a plicated integument (PI), which represents the epithelium layer, a connective tissue layer containing granulocytes (GC), was observed. In addition, a somatic musculature (SM) layer was seen in normal tissue. Ciliated columnar epithelial cells (CEC) and mucous cells made up the plicated integument. In contrast, the mantle's musculature layer has longitudinal cross-sections of myocytes (Figure 6). After exposure to ZnO NPs and ZnO/Alg NCs, severe degenerative alterations in the mantle, including muscle bundle breaking, severe muscular atrophy, and granulocyte enlargement, were observed. Despite being observed for both substances, the effect was more pronounced in tissues treated with ZnO/Alg NCs.

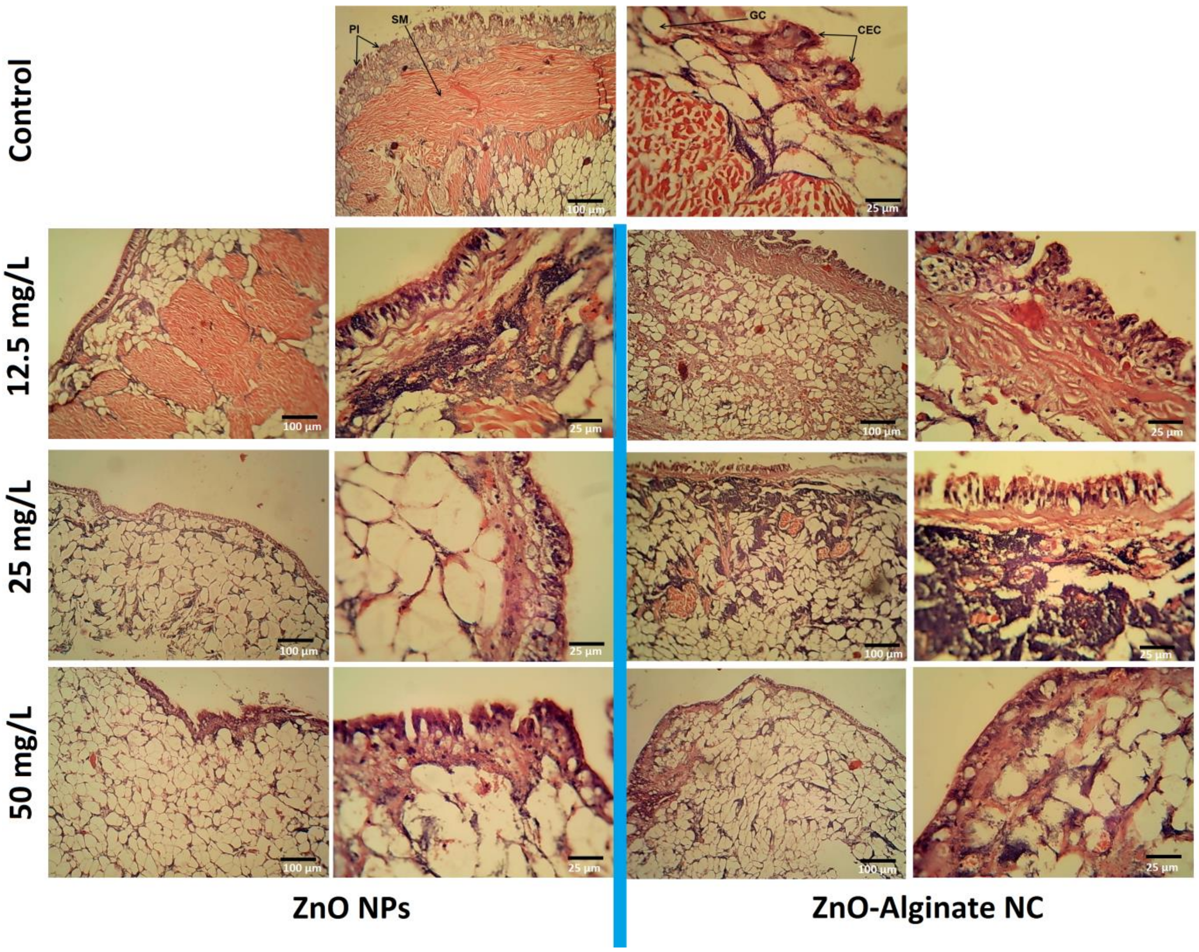

Figure 6. Light micrographs of the mantle of *Coelatura aegyptiaca* exposed to ZnO NPs and ZnO/Alg NC NCs (H&E). "GC" granulocytes, "CEC" ciliated columnar epithelial cells, "SM" somatic musculature, and "PI" plicated integument.

4. Conclusions

In this study, freshwater bivalves were exposed to ZnO NPs and ZnO/Alg NCs, which resulted in oxidative stress responses and histological alterations in their gills and mantle. These physiological and histological changes reported after exposure to ZnO/Alg NCs were almost more striking than those seen after exposure to ZnO NPs. *Coelatura aegyptiaca* was found to be a sensitive bioindicator for monitoring nanoparticle-related water pollution. As a result, it is recommended that ZnONPs be utilized with greater caution in relevant industries and address occupational health surveillance.

Funding

No funding sources.

Acknowledgments

The authors extend their appreciation to the Deanship of Scientific Research at Cairo University, Egypt, for supporting the current work.

Conflicts of Interest

The authors declare no conflict of interest.

5. References

1. Rani, A.; Suri, P.; Shishodia, P.K.; Mehra, R.M. Synthesis of nanocrystalline ZnO powder via sol–gel route for dye-sensitized solar cells. *Solar Energy Materials and Solar Cells* **2008,** *92*, 1639-1645, https://doi.org/10.1016/j.solmat.2008.07.015.
2. Sharma , D.; Sharma , S.; Kaith, B. S.; Rajput, J.; Kaur, M. Synthesis of ZnO nanoparticles using surfactant free in-air and microwave method. *Applied Surface Science* **2011,** *257*, 9661- 9672, https://doi.org/10.1016/j.apsusc.2011.06.094.
3. Iwasaki, M.; Inubushi, Y.; Ito, S. New route to prepare ultrafine ZnO particles and its reaction mechanism. *Journal of Materials Science Letters* **1997,** *16*, 1503–1505.
4. Calzoni, E.; Cesaretti, A.; Polchi, A.; Di Michele, A.; Tancini, B.; Emiliani, C. Biocompatible Polymer Nanoparticles for Drug Delivery Applications in Cancer and Neurodegenerative Disorder Therapies. *Journal of functional biomaterials* **2019,** *10*, 4, https://doi.org/10.3390/jfb10010004.
5. Sorasitthiyanukarn, F.N.; Muangnoi, C.; Rojsitthisak, P.; Rojsitthisak, P. Chitosan-alginate nanoparticles as effective oral carriers to improve the stability, bioavailability, and cytotoxicity of curcumin diethyl disuccinate. *Carbohydrate polymers* **2021,** *256*, 117426, https://doi.org/10.1016/j.carbpol.2020.117426.
6. Lian, Y.; Wang, X.; Guo, P.; Li, Y.; Raza, F.; Su, J.; Qiu, M. Erythrocyte Membrane-Coated Arsenic Trioxide-Loaded Sodium Alginate Nanoparticles for Tumor Therapy. *Pharmaceutics* **2019,** *12*, 21, https://doi.org/10.3390/pharmaceutics12010021.
7. Asztemborska, M.; Jakubiak, M.; Stęborowski, R.; Chajduk, E.; Bystrzejewska-Piotrowska, G. Titanium Dioxide Nanoparticle Circulation in an Aquatic Ecosystem. *Water Air Soil Pollut* **2018,** *229*, 208, https://doi.org/10.1007/s11270-018-3852-8.
8. Maynard, A.D. Nanotechnology: The Next Big Thing, or Much Ado About Nothing? *Ann. Occup. Hyg* **2007,** *51*, 1–12, https://doi.org/10.1093/annhyg/mel071.
9. Gökçe, D. Influences of nanoparticles on aquatic organisms: Current situation of nanoparticles effects in aquatic ecosystems. *Sustainable Engineering and Innovation* **2021,** *3*, 54-60, https://doi.org/10.37868/sei.v3i1.id136.
10. Bundschuh, M.; Filser, J.; Lüderwald, S.; McKee, M.S.; Metreveli, G.; Schaumann, G.E.; Schulz, R.; Wagner, S. Nanoparticles in the environment: where do we come from, where do we go to? *Environ Sci Eur* **2018,** *30*, 6, https://doi.org/10.1186/s12302-018-0132-6.
11. Khan, B.; Ho, K. T.; Burgess, R.M. Application of Biomarker Tools Using Bivalve Models Toward the Development of Adverse Outcome Pathways for Contaminants of Emerging Concern. *Environmental Toxicology and Chemistry* **2020,** *39*, 1472-1484, https://doi.org/10.1002/etc.4757.
12. Radwan, E.H.; Mawgood, A.A.; Ghonim, A.Z.; Nagar , R.E. The Possibility of Using the Fresh Water Bivalve, Spathopsis Rubens, in The Nile River, El Mahmoudia Water Stream as Bioindicator For Pollution. *International Journal of Limnology* **2018,** *1*, 1-23, https://doi.org/10.14302/issn.2691-3208.ijli-18-2476.
13. Mohamed, A.S.; Ibrahim, W.I.; Zaki, N.I.; Ali, S.B.; Soliman, A.M. Effectiveness of *Coelatura aegyptiaca* Extract Combination with. *Evidence-Based Complementary and Alternative Medicine* **2019,** *2019*, 9, https://doi.org/10.1155/2019/9726137.

14. Cao, D.; Gong, S.; Shu, X.; Zhu, D.; Liang, S. Preparation of ZnO Nanoparticles with High Dispersibility Based on Oriented Attachment (OA) Process. *Nanoscale Research Letters* **2019,** *14*, 210, https://doi.org/10.1186/s11671-019-3038-3.
15. Tamer, T.M.; Abou-Taleb, W.M.; Roston, G.D.; Mohyeldin, M.S.; Omer, A.M.; Khalifa, R.E.; Hafez, A.M. Formation of zinc oxide nanoparticles using alginate as a template for purification of wastewater. *Environmental Nanotechnology, Monitoring & Management* **2018,** *10*, 112-121, https://doi.org/10.1016/j.enmm.2018.04.006.
16. Mohamed, A.S.; Elkareem, M.A.M.; Soliman, A.M.; Fahmy, S.R. Potential inhibition of ehrlich ascites carcinoma by naja nubiae crude venom in swiss albino mice. *Biointerface Research in Applied Chemistry* **2022,** *12*, 7741 – 7751, https://doi.org/10.33263/BRIAC126.77417751.
17. Youssef, A.; Baiomy, A.; Fahmy, S.R.; Mohamed, A.S.; Saad, D.; Desoky, R. Potential anti-osteoporotic effect of Allolobophora caliginosa extract in orchiectomized rats. *Pharmaceutical Sciences Asia* **2022,** *49*, 138 – 146, https://doi.org/10.29090/psa.2022.02.21.144.
18. Beutler, E.; Duron, O.; Kelly, M.B. Improved method for the determination of blood glutathione. *Journal of Laboratory and Clinical Medicine* **1963,** *61*, 882–888.
19. Aebi, H. Catalase *in vitro*. *Methods in Enzymology* **1984,** *105*, 121-126.
20. Montgomery, H.A.C.; Dymock, J.F. The determination of nitrite in water. *Analyst.* **1961,** *86*, 414–416.
21. Lotfy, B.M.M.; Mousa, M.R.; El-Shehry, M.S.F.E.; Ahmed, S.H.A.; Ali, S.B.; Al Shawoush, A.M.; Mohamed, A.S. Therapeutic Potency of Gallium verum Extract on Ethanol-Induced Gastric Ulcer in Rats. *Biointerface Research in Applied Chemistry* **2022,** *12*, 6010 – 6020, https://doi.org/10.33263/BRIAC125.60106020.
22. Magdy, A.; Fahmy, S.R.; Mohamed, A.S.; Saad, D.Y.; Desoky, R.S.; Baiomy, A.A. Histopathological and Immunohistochemical Study of Antiosteoporotic Efficacy of the Earthworm Allolobophora caliginosa Extract in Orchiectomized Rats. *International Journal of Morphology* **2022,** *40*, 277 - 286.
23. Srikanth, K.; Raju, N.V.; Pamanji, R.; Nutalapati, V. Pila virens as sentinel of silica nanoparticles toxicity induced oxidative stress. *Materials Letters* **2021,** *300*, 130185, https://doi.org/10.1016/j.matlet.2021.130185.
24. Mamdouh, S.; Mohamed, A.S.; Mohamed, H.A.; Fahmy, W.S. Zn contamination stimulate agonistic behavior and oxidative stress of crayfishes (Procambarus clarkii). *Journal of Trace Elements in Medicine and Biology* **2022,** *69*, 126895, https://doi.org/10.1016/j.jtemb.2021.126895.
25. Mamdouh, S.; Mohamed, A.S.; Mohamed, H.A.; Fahmy, W.S. The Effect of Zinc Concentration on Physiological, Immunological, and Histological Changes in Crayfish (Procambarus clarkii) as Bio-indicator for Environment Quality Criteria. *Biological Trace Element Research* **2022,** *200*, 375–384, https://doi.org/10.1007/s12011-021-02653-x.
26. Kahru , A.; Dubourguier, H.C. From ecotoxicology to nanoecotoxicology. *Toxicology* **2010,** *269*, 105–119, https://doi.org/10.1016/j.tox.2009.08.016.
27. Vimercati, L.; Cavone, D.; Caputi, A.; De Maria, L.; Tria, M.; Prato, E.; Ferri, G.M. Nanoparticles: An Experimental Study of Zinc Nanoparticles Toxicity on Marine Crustaceans. General Overview on the Health Implications in Humans. *Frontiers in Public Health* **2020,** *8*, 1–19, https://doi.org/10.3389/fpubh.2020.00192.
28. Vale, G.; Mehennaoui, K.; Cambier, S.; Libralato, G.; Jomini, S.; Domingos, R.F. Manufactured nanoparticles in the aquatic environment-biochemical responses on freshwater organisms: a critical overview. *Aquatic Toxicology* **2016,** *170*, 162–174, https://doi.org/10.1016/j.aquatox.2015.11.019.
29. Bin Dajem, S.; Ali, S.B.; Abdelrady, O.G.; Salahaldin, N.M.; Soliman, A.M.; Kamal, Y.M.; Abdelazim, A. Y.; Mohamed, A.F.; Morsy, K.; Mohamed, A.S.; Fahmy, S.R. Allolobophora caliginosa coelomic fluid ameliorates gentamicin-induced hepatorenal toxicity in rats. *Asian Pacific Journal of Tropical Biomedicine* **2020,** *10*, 411-416, https://doi.org/10.4103/2221-1691.290132.
30. Mohamed, A.S.; Al-Quraishy, S.; Abdel-Gaber, R.; Fahmy, S.R. Silver/Chitosan/Ascorbic Acid Nanocomposites Attenuates Bacterial Sepsis in Cecal Ligation and Puncture Rat Model. *International Journal of Pharmacology* **2021,** *17*, 549-561, https://doi.org/10.3923/ijp.2021.549.561.
31. Mohamed, A.S.; Bin Dajem, S.; Al-Kahtani, M.; Ali, S.B.; Alshehri, M.; Shati, A.; Morsy, K.; Fahmy, S.R. Freshwater Clam as a Potential Bioindicator for Silver/Saponin. *Bulletin of environmental contamination and toxicology* **2020,** *105*, 827-834, https://doi.org/10.1007/s00128-020-03038-x.
32. El-Sisi, A.A.; Fahmy, S.R.; El-Desouky, M.A.; El-Tawil, O.; Mohamed, A.S.; El-Sherif, A.A. Protective roles of novel thiosemicarbazone derivatives on hepatotoxicity and nephrotoxicity induced by cadmium

chloride in rats. *Acta Poloniae Pharmaceutica - Drug Research* **2021,** *78*, 193–203, https://doi.org/10.32383/appdr/135247.
33. Özel, R.E.; Alkasir, R.S.J.; Ray, K.; Wallace, K.N.; Andreescu, S. Comparative Evaluation of Intestinal Nitric Oxide in Embryonic Zebrafish Exposed to Metal Oxide Nanoparticles. *small* **2013,** *9*, 4250–4261, https://doi.org/10.1002/smll.201301087.
34. Mohamed, A.S.; Bin Dajem, S.; Al-Kahtani, M.; Ali, S.B.; Ibrahim, E.; Morsy, K.; Fahmy, S.R. Silver/chitosan nanocomposites induce physiological and histological changes in freshwater bivalve. *Journal of Trace Elements in Medicine and Biology* **2021,** *65,* 126719, https://doi.org/10.1016/j.jtemb.2021.126719.
35. Sadek, S.A.; Hassanein, S.S.; Mohamed, A.S.; Soliman, A.M.; Fahmy, S.R. Echinochrome pigment extracted from sea urchin suppress the bacterial activity, inflammation, nociception, and oxidative stress resulted in the inhibition of renal injury in septic rats. *Journal of food biochemistry* **2021,** *2021*, e13729. https://doi.org/10.1111/jfbc.13729.
36. Bahaaeldine, M. A.; El Garhy, M.; Fahm, S. R.; Mohamed, A. S. *In vitro* anti-Toxocara vitulorum effect of silver nanoparticles. *J Parasit Dis* **2022,** *2022,* 50-58, https://doi.org/10.1007/s12639-021-01464-0.
37. Dubey, A.; Goswami, M.; Yadav, K.; Chaudhary , D. Oxidative Stress and Nano-Toxicity Induced by TiO2 and ZnO on WAG Cell Line. *PLoS One* **2015,** *10*, e0127493, https://doi.org/10.1371/journal.pone.0127493.
38. Mohamed, A.S. Echinochrome Exhibits Antitumor Activity against Ehrlich Ascites Carcinoma in Swiss Albino Mice. *Nutrition and Cancer* **2021,** *73*, 124-132, https://doi.org/10.1080/01635581.2020.1737152.
39. Mohamed, A. S.; Fahmy, S. R.; Soliman, A. M.; Gaafar, K. M. Effects of 3 Rodent Beddings on Biochemical Measures in Rats and Mice. *Journal of the American Association for Laboratory Animal Science* **2018,** *57*, 443-446, https://doi.org/10.30802/AALAS-JAALAS-18-000023.
40. Madany, N.M.K.; Shehata, M.R.; Mohamed, A.S. Ovothiol-a isolated from sea urchin eggs suppress oxidative stress, inflammation, and dyslipidemia resulted in restoration of liver activity in cholestatic rats. *Biointerface Research in Applied Chemistry* **2022,** *12*, 8152 – 8162, https://doi.org/10.33263/BRIAC126.81528162.